Flutter analysis of laminated composite structures using Carrera Unified Formulation

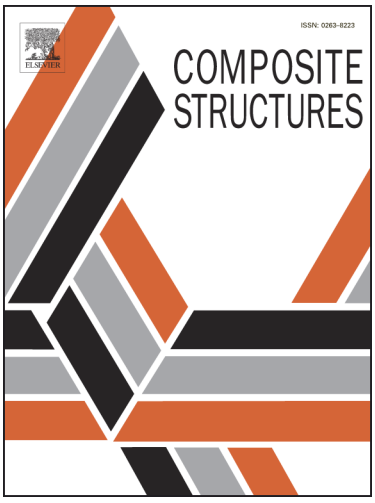

Flutter analysis of laminated composite structures using Carrera Unified Formulation

Raj B. Bharati, M. Fillipi, Prashanta K. Mahato, E. Carrera

PII: S0263-8223(20)32685-4
DOI: https://doi.org/10.1016/j.compstruct.2020.112759
Reference: COST 112759

To appear in: *Composite Structures*

Received Date: 26 May 2020
Accepted Date: 28 July 2020

Please cite this article as: Bharati, R.B., Fillipi, M., Mahato, P.K., Carrera, E., Flutter analysis of laminated composite structures using Carrera Unified Formulation, *Composite Structures* (2020), doi: https://doi.org/10.1016/j.compstruct.2020.112759

Flutter analysis of laminated composite structures using Carrera Unified Formulation

Raj B. Bharati[a,b,1], M. Fillipi[a,2], Prashanta K. Mahato[b,3,*], E. Carrera[a,4]

[a] *MUL^2 Group, Department of Mechanical and Aerospace Engineering, Politecnico di Torino, Turin, Italy*

[b] *Department of Mechanical Engineering, Indian Institute of Technology (Indian School of Mines), Dhanbad, India*

Abstract

In present work, the flutter analysis of laminated composite structures has been performed using the *p-k* method in Carrera Unified Formulation (CUF). In the framework of CUF, a hierarchical kinematic finite element model is used to compute the flutter condition of laminated composite plate and box-beam structures as it is very accurate and computationally efficient. The CUF refined theories are based on the Lagrange and Taylor-like cross-sectional displacement fields. In CUF, the order of the expansion can be chosen arbitrary, which is an independent parameter in the formulation. The governing equation is based on the principle of virtual displacement and defined in the form of "fundamental nuclei" using CUF. Theodorsens theory was used to define the aerodynamics loading conditions and the *p-k* method was used to compute the flutter conditions. Flutter conditions of different types of laminated composite structures with Lagrange and Taylor expansion were performed. A similar model was developed in MSC-Nastran and computed results were compared with literature and CUF model. The results indicate that the analyzed model has good agreement with reference

*Corresponding author

Email addresses: raj.bharati@polito.it (Raj B. Bharati), matteo.filippi@polito.it (M. Fillipi), pkmahato@iitism.ac.in (Prashanta K. Mahato), erasmo.carrera@polito.it (E. Carrera)

[1] PhD. Student

[2] Assistant Professor

[3] Associate Professor

[4] Professor of Aerospace Structures and Aeroelasticity

and MSC-Nastran. The study suggests that the CUF models can produce accurate results with a low computational cost.

Keywords: Flutter, Unified Formulation, p-k method, Composites

1. Introduction

Flutter is a dynamic instability found in a different kind of flexible structure like air-vehicles, bridges, and blades. It can introduce the catastrophic failure of the structure. It is a devastating reason for failure, and most anxiety subject to the designer. So, the flutter should be considered and thoroughly analyzed during the design process of the aircraft structure. Several authors have analyzed the aeroelastic behavior of aircraft structure since Theodorsen developed a mechanism for the flutter analysis and demonstrated the flutter problem theoretically and experimentally [1, 2]. Later many methods have been developed to solve the flutter problem and improve the solution methodology such as v-g method, k-method and p-k method [3, 4].

Now-a-days, the laminated composite structures are broadly used in the design process of modern air vehicles, bridges and blades, owing to their high structural efficiency, specific strength and potential benefits. The wings can be modeled as the isotropic and thin-walled composite beam [5]. It can also be modeled as the laminated composite beam for the finite element solution to performed the free vibration analysis [6]. For further extension, the laminated composite beam can be considered as the thin- and thick-walled box-beam model for experimental, analytical and numerical solutions in order to determine the elastic stiffness, tailoring effect and torsional warping in finite element approach [7, 8, 9].

The laminated composite structures are very much flexible and aeroelastic behavior of these flexible structures should be analyzed to avoid flutter failure. For the prediction of flutter condition and divergence behavior of these structures, the combination of strip theory with simplified structural box-beam models was analyzed [10]. Various parameters such as aspect ratio, stacking sequences and sweep angle are considered for aeroelastic tailoring [11]. The analytical approach has been used to find the flutter condition for the wing made of the composite material [12]. In the aeroelastic investigation of a structure made with anisotropic composite, directionality property played a complex role in predicting the flutter and divergence behavior [13]. The analytical approach also used for the box-beam model and aeroelas-

tic optimization have been studied [14, 15]. The aeroelastic characteristics of laminated plate have been observed for various lamination parameters, aspect ratio, material properties and sweep angle and found different aeroelastic parameters (flutter/divergence) at the same speed of air (free stream) [16]. The Theodorsen theory can be used for quasi-steady and unsteady aerodynamics to compute the flutter. Several authors predicted the flutter condition using the Theodorsen theory along with various approaches (such as strip theory and panel method) [17, 18, 19, 20]. To improve the flutter solution, Hassig [4] proposed the p-k method that can provide better approximation than the other methods [21]. This method also can be used for the smart laminated plate in hygrothermal environment [22].

The aim of this work is to develop a finite element model of laminated composite structures (plate and box-beam) using Carrera Unified Formulation (CUF) and to perform flutter analysis by the p-k method. The different kinds of complex laminated composite structural models have been considered and those types of the model required proper description of the kinematics, which are defined accurately and computationally efficient manner in CUF. Initially, CUF was developed to deal with a plate and shells [23, 24, 25] later, it was extended and to deal with the beam model [26, 27]. The CUF has a unique capability such as the order of Taylor expansion can be chosen arbitrarily to define the cross-sectional displacement fields. These capabilities give us freedom to choose the order of structural models without making changes in matrices or equations and without the need of any ad hoc formulation, it can deal with arbitrary geometry, different material characteristics, and boundary conditions. This present approach is computationally efficient for different kinds of structures such as thin-walled [28], laminated and sandwich structure [29]. It can be used for rotating blades [30] and spinning blades [31] in the rotor dynamics fields. In the field of fluid interaction, CUF has been used for vortex [32, 33, 34] and double lattice method [35, 36], and piston theory [37, 38] for supersonic flows. Recently, [39] the coupling of CUF with the Theodorsen theory has been done to predict the flutter condition by the v-g method. In this work, the p-k method has been implemented in CUF framework to analyze the flutter condition.

2. Structural Model: Carrera Unified Formulation

The present structural model formulated within the popular Carrera Unified Formulation (CUF) framework [40, 41, 42, 43, 44]. In accordance with

CUF, u is defined as the displacement fields which can be stated as a combination of the $F_\tau(x,z)$ (function of cross-section) and $u_\tau(y)$ displacement vector (generalized), and can unify as:

$$u(x,y,z,t) = F_\tau(x,z)u_\tau(y), \quad \tau = 1,2,....,T \tag{1}$$

where subscript τ and T stands for summation (i.e. Einstein notation) and the number of terms in the expansion, respectively. The details of Taylor expansion (TE) and displacement fields are given in Table 1.

Table 1: Compact form and displacement fields of Taylor expansion.

Order	T	F_τ	Displacement fields
0	1	$F_1 = 1$	Second-order (TE2)
1	3	$F_2 = x\ F_3 = z$	$u_x = u_{x_1} + x\ u_{x_2} + z\ u_{x_3} + x^2\ u_{x_4} + xz\ u_{x_5} + z^2\ u_{x_6}$
2	6	$F_4 = x^2\ F_5 = xz\ F_6 = z^2$	$u_y = u_{y_1} + x\ u_{y_2} + z\ u_{y_3} + x^2\ u_{y_4} + xz\ u_{y_5} + z^2\ u_{y_6}$
3	10	$F_7 = x^3\ F_8 = x^2z\ F_9 = xz^2\ F_{10} = z^3$	$u_z = u_{z_1} + x\ u_{z_2} + z\ u_{z_3} + x^2\ u_{z_4} + xz\ u_{z_5} + z^2\ u_{z_6}$
⋮	⋮	⋮	
N	(N+1) (N+2) / 2	$F_{(N+1)(N+2)/2} = x^N\ F_{(N+1)(N+2)/2} = z^N$	

Two types of CUF models are used in this present work: Taylor expansion (TE) and Lagrange expansion (LE). The TE model is refined by increasing the order of expansion from second-order (TE2) to fourth-order (TE4). Similarly, LE is refined by adding the elements in the cross-section, i.e., one nine-noded (1L9) and two nine-noded (2L9) along the chord. The details of the displacement fields of the LE model can be found in literature [44]. Cross-sectional elements are extended along the y-axis with four-noded beam elements (B4) to create the structure (Figure 1).

3. Aeroelastic Model: Steady and Unsteady Theories

A complete solution of a thin airfoil in the incompressible fluid, which is associated with the harmonic oscillations laterally, Theodorsen's presented the lift distribution function by going beyond the quasi-steady model. He considered a control surface of a plate that was assumed as flat, which can rotate with regard to an axis at distance $x = b_c a$ via the angle of attack $\Lambda(t)$ and move vertically $h(t)$. Theodorsen's unsteady lift prediction expression is

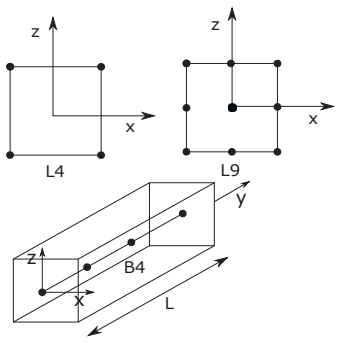

Figure 1: Four- and nine-nodes Lagrange elements and four-nodes beam element.

[45]:

$$L_a = \pi\rho_a b_c^2 \left[\ddot{h} + V_\infty\dot{\alpha} - b_c a\ddot{\alpha}\right] + 2\pi\rho_a b_c C(k) V_\infty \left[\dot{h} + V_\infty\alpha + b_c\left(\frac{1}{2} - a\right)\dot{\alpha}\right] \tag{2}$$

where ρ_a is air density, b_c is semi-chord, V_∞ is free-stream velocity and Theodorsen function $C(k)$ is the relating the reduced frequency $k = \dfrac{\omega b_c}{V_\infty}$. The position of the axis of rotation with regard to the center of section denoted as a, which depends on the load applied, used lamination scheme and support condition. The first term of equation (2) is the non-circulatory (i.e., added mass term), whereas the second term is the circulatory. The second term is called "quasi-steady" model when Theodorsen function $\{C(k) = 1\}$ and "unsteady aerodynamics" when Theodorsen function is a complex function $C(k) = F(k) + iG(k)$. The simplified expression of $C(k)$ has been presented by Jones [46] by considering the solution of Wagners indicial (1925), which was concerned to exponential approximation:

$$C(k) \equiv 1 - \frac{0.165}{1 - \left(\dfrac{0.0455}{k}\right) i} - \frac{0.335}{1 - \left(\dfrac{0.3}{k}\right) i} \tag{3}$$

The first term of equation (2) can be neglected due to mass properties of the structure are small and it is related to single and double differentiated terms and can be written as:

$$L_a \equiv 2\pi\rho_a V_\infty b_c \left[\dot{h} + V_\infty\alpha\right] \tag{4}$$

For correcting the coefficient of C_L (sectional lift) associated with an aspect ratio of the wing (AR_w) and sweep angle (Λ) effects, by using Diederich's approximation, the expression becomes:

$$C_{l\alpha} = \frac{dC_L}{d\alpha} = \frac{\pi AR_w}{\pi AR_w + C_{l\alpha 0} cos(\Lambda)} C_{l\alpha 0} cos(\Lambda) \tag{5}$$

where, $(AR_w) = \dfrac{2\ L_w}{c_m}$, ($L_w$ = wing length and C_m =mean chord) [Figure 2], and $C_{l\alpha 0}$ is stated as slope of lift-curve ($\approx 2\pi$). In order to reproduce the pressure distribution on atop of airfoil, which is thin, slightly inclined and uncambered. For capturing the effect of pressure distribution on concerned geometry of the wing model, the quantity of $b_c\pi$ has been approximated by $\int_{-b_c}^{b_c} \sqrt{\dfrac{b_c - x}{b_c + x}} dx$, and equations (2) and (4) can be rewritten as:

$$L_a = \frac{2\pi\ AR_w\ cos(\Lambda)}{\pi\ AR_w + 2\pi\ cos(\Lambda)} \int_{-b_c}^{b_c} \sqrt{\frac{b_c - x}{b_c + x}} dx \rho_a V_\infty c(k) \left[\dot{h} + V_\infty \alpha + b_c \left(\frac{1}{2} - a \right) \dot{\alpha} \right] \tag{6}$$

$$L_a \equiv \frac{2\pi\ AR_w\ cos(\Lambda)}{\pi\ AR_w + 2\pi\ cos(\Lambda)} \int_{-b_c}^{b_c} \sqrt{\frac{b_c - x}{b_c + x}} dx\ \rho_a V_\infty c(k)\ [\dot{h} + V_\infty \alpha] \tag{7}$$

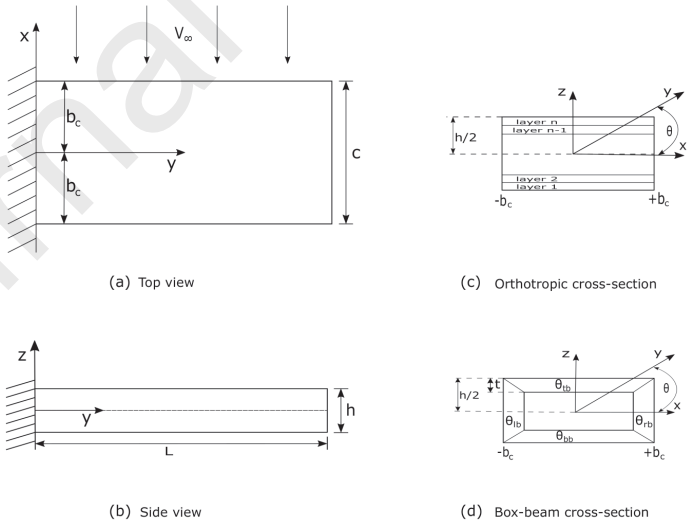

Figure 2: Sketch of beam model and coordinates reference system.

4. Formulation of equation of motion: CUF framework

The equation of motion for aeroelastic model has been derived using the principle of virtual displacement (PVD), stated as below:

$$\delta L_{int} = \delta L_{ext} + \delta L_{ine} \tag{8}$$

where δL_{int} (internal work), δL_{ext} (external work), δL_{ine} (inertial work) and δ stands for virtual variation.
The strain and kinetic energy can be write in the form of fundamental nuclei as follow:

$$\delta L_{int} = \delta q_{\tau i}^{T} \, K_{s}^{ij\tau s} \, q_{sj}, \tag{9}$$

$$\delta L_{ine} = \delta q_{\tau i}^{T} \, M_{s}^{ij\tau s} \, \ddot{q}_{sj} \tag{10}$$

where $K_{s}^{ij\tau s}$ and $M_{s}^{ij\tau s}$ defined as a fundamental nucleus for the stiffness and mass matrix, respectively and components are found in literature [47].
The generalized form of the work produced by the lift is:

$$\delta L_{ext} = \int_{y} \int_{x} \delta u_z(x, y, z_{top}) L_a(x, y, z_{top}) dx dy \tag{11}$$

where z_{top} is associated with upper coordinate of a cross-section in z and L is lift given in equation (7). In Carrera Unified Formulation framework, external work can be written as:

$$\delta L_{ext} = \delta q_{\tau i}^{T} \, D_{L}^{ij\tau s} \, \dot{q}_{sj} + \delta q_{\tau i}^{T} \, K_{L}^{ij\tau s} \, q_{sj} \tag{12}$$

where $D_{L}^{ij\tau s}$ (damping) and $K_{L}^{ij\tau s}$ (stiffness) are contributions due to the aerodynamic force, which are defined in fundamental nuclei form:

$$\begin{aligned} D_{L}^{ij\tau s} &= cost \; I_{l}^{ij} \int_{-b_c}^{b_c} \sqrt{\frac{b_c - x}{b_c + x}} F_{\tau}(x, z_{top}) \; I_L \; F_s(x, z_{top}) \; dx \\ K_{L}^{ij\tau s} &= cost \; I_{l}^{ij} \int_{-b_c}^{b_c} \sqrt{\frac{b_c - x}{b_c + x}} F_{\tau,x}(x, z_{top}) \; I_L \; F_s(x, z_{top}) \; dx \end{aligned} \tag{13}$$

where

$$cost = \frac{2\pi \; AR_w \; cos(\Lambda)}{\pi \; AR_w + 2\pi \; cos(\Lambda)} \; \rho_a V_{\infty} c(k) \tag{14}$$

$$I_L = \begin{bmatrix} 0 & 0 & 0 \\ 0 & 0 & 0 \\ 0 & 0 & 1 \end{bmatrix} \tag{15}$$

$$I_l^{ij} = \int_l N_i N_j \, dy \tag{16}$$

After assembly of global finite element matrices by assuming the periodic solution $a_q = \bar{a}_q e^{i\omega t}$ in the form of quadratic eigenvalue problem (QEP) and transforming into classical liner system of $2 \times R$ can we write as:

$$\begin{cases} [M_s]\ddot{a_q} + [D_L]\dot{a_q} + ([K_s] + [K_L])a_q = 0 \\ -\dot{a_q} + \dot{a_q} = 0 \end{cases} \tag{17}$$

and by presenting:

$$a = \begin{Bmatrix} a_q \\ \dot{a_q} \end{Bmatrix}, \quad \dot{a} = \begin{Bmatrix} \dot{a_q} \\ \ddot{a_q} \end{Bmatrix} \tag{18}$$

equation of motion assumed in the following form:

$$\frac{R}{T} - \frac{1}{i\omega} I = 0, \tag{19}$$

where

$$I^{-1}R = \begin{bmatrix} (K + K_L)^{-1} D_L & (K + K_L)^{-1} M \\ -I & 0 \end{bmatrix} \tag{20}$$

An iterative procedure was required to calculate the flutter condition because of aerodynamic contribution matrices, which have a dependency on the reduced frequency (k). The p-k method proposed by Hassig [4] is used for solving the flutter problem. The General form of a proposed equation given as:

$$\left[\left(\frac{V_\infty}{c_m} \right)^2 [M_s]p^2 + [K_s] - \frac{1}{2}\rho V_\infty^2 [A(p)] \right] \{a_q\} = 0 \tag{21}$$

where, $[A(p)]$ = unsteady aerodynamic forces. The Simplified fundamental equation for modal flutter analysis presented in [48]:

$$\left[[[M_s]\, p^2 + \left([B_s] - \frac{1}{4}\rho c V_\infty \frac{[Q_a^I]}{k} \right) p + [K_s] - \frac{1}{2}\rho V_\infty^2 [Q_a^R] \right] \{a_q\} = 0 \tag{22}$$

where, $[Q_a^I]$,$[Q_a^R]$ are imaginary and real part of aerodynamic force matrix, c is reference length, p is eigenvalue, k reduced frequency and $[B_s] = 0$ because structural damping is not considered here. The circular frequency ω and reduced frequency k are not independent since $k = \dfrac{\omega b_c}{V_\infty}$,

$$k = \frac{b}{V_\infty} im(p) \tag{23}$$

and

$$p = \gamma\omega + i\omega \tag{24}$$

where, γ is transient decay rate coefficient ($2\gamma = g$).

5. Results And Discussion

Based on the above formulation, a FORTRAN finite element model is developed to analyze the flutter condition of laminated composite structures (plate and box-beam) model. Carrera Unified Formulation (CUF) has a hierarchical finite element model, which is very accurate and economically efficient. In CUF, we can choose any order of Taylor's expansion without changing in the formulation. Plate elements (CQUAD4) based on the Mindlin-Reissner shell theory are used to develop the MSC-Nastran model (i.e., isotropic, orthotropic and box-beam) for the comparison of results obtained by CUF. Numerical examples of isotropic and laminated composite structures are presented in subsequent sections. The flutter condition of both models is computed by using the p-k method and flutter condition (flutter velocity) is defined at the point where the real part of the eigenvalue (damping) is null.

5.1. Isotropic plate

The first numerical example is based on the work of Petrolo [49]. Where a cantilever straight plate with the geometrical data: length $L = 0.305$ m, thickness $t = 0.001$ m, and chord $c = 0.076$ m, having isotropic material properties: $E = 73.8$ GPa, $\nu = 0.3$ and $\rho = 2768$ Kg/m^3 has been analyzed. The flutter analysis of the plate model using CUF based finite element method (FEM) and MSC-Nastran model with sweep angle $\lambda = 0^\circ$ has been performed. The different orders of Taylor expansion (TE) and Lagrange expansion (LE) with nine-noded (L9) cross-sectional elements have been considered for CUF

model to compute the results. The first five modes (i.e., bending and torsion) of natural frequency (f_n), flutter velocity (V_F), and flutter frequency (f_F) of CUF and MSC-Nastran model are reported in Table 2. MSC-Nastran model was created using the plate elements (CQUAD4) with 8x20 grids. The computed flutter velocity and frequency using the *p-k* method are compared with MSC-Nastran and results obtained using the doubled-lattice method of literature. It is observed that the modal frequencies are matching well with MSC-Nastran. Also, observed that modal frequencies and flutter conditions of third-order Taylor expansion (TE3), fourth-order (TE4), and two nine-noded LE model are more accurate for the present isotropic plate and the desired result is achieved with a very low computational cost.

Table 2: Natural frequencies (Hz) and flutter conditions.

	Model	Mesh	DOFs	f_{n_1}	f_{n_2}	f_{n_3}	f_{n_4}	f_{n_5}	V_F (m/s)	f_F (Hz)
Reference [49]	TE4	20B4							72.75	59.77
Present	TE2	12B4	666	9.40	58.84	74.21	165.10	230.81	75.70	42.05
	TE3	12B4	1110	9.14	57.19	73.71	160.60	227.94	71.60	39.63
	TE4	12B4	1665	9.14	57.16	73.70	160.52	227.77	69.80	39.15
	LE (1L9)	12B4	999	9.14	57.17	73.72	160.54	227.97	74.90	40.47
	LE (2L9)	12B4	1665	9.14	57.17	73.70	160.53	227.74	70.70	39.41
	MSC-Nastran	8x20	945	9.09	56.74	72.12	158.95	222.07	66.51	39.52

5.2. Orthotropic plate

A six-layered laminated composite plate is considered in this section with symmetric laminate $[30_2/0]_s$. The cantilever plate with length ($L = 0.305$ m), chord ($c = 0.0762$ m) and thickness ($t = 0.000804$ m) having material properties $E_L = 98.00$ GPa, $E_T = 7.90$ GPa, $G_{LT} = 5.60$ GPa, $\nu = 0.280$, and $\rho = 1520.00$ kg/m^3 has been analyzed to find flutter conditions. The different orders of Taylor expansions, e.g., second-order (TE2), third-order (TE3) and fourth-order (TE4) used to describe the cross-section of a plate. Similarly, two types of Lagrange elements, one nine-noded (1L9) and two nine-noded (2L9), along with the chord used to defined the cross-section of a single layer. The first five modes of natural frequency and flutter condition for the $[30_2/0]_s$ plate are reported in Table 3. The mode shapes of bending and torsion for LE (2L9) model are shown in Figure 3. Computed results indicate that TE3,

TE4 and 2L9 produce more accurate results as compared to TE2 and 1L9. The first five modes of frequencies and damping with respect to functions of speed for the present CUF (TE3) and MSC-Nastran model are plots in Figure 4. The various stacking sequence $[0_2/90]_s$, $[45/-45/0]_s$ and $[45_2/0]_s$ are used to compute flutter conditions for TE3 and 2L9 models, which are reported in Table 4. Here results show that different stacking sequences can influence both natural frequency and flutter conditions.

Table 3: Natural frequencies (Hz) and flutter conditions for a laminated plate (6-layers) $[30_2/0]_s$.

	Model	Mesh	DOFs	f_{n_1}	f_{n_2}	f_{n_3}	f_{n_4}	f_{n_5}	V_F (m/s)	f_F (Hz)
Reference [36]	TE4	15B4	2070	6.05	35.91	56.51	100.03	172.23	25.86	26.66
Present	TE2	10B4	558	6.34	37.91	69.43	107.43	213.96	31.90	28.38
	TE3	10B4	930	6.31	37.49	57.73	104.65	178.90	27.80	27.90
	TE4	10B4	1395	6.21	37.25	56.94	103.76	173.82	27.60	27.22
	LE (1L9)	10B4	3627	6.31	37.52	57.77	104.72	179.11	29.50	27.59
	LE (2L9)	10B4	6045	6.30	37.33	57.11	104.04	174.68	28.10	27.10
	MSC-Nastran	10x30	1705	6.26	37.05	55.97	103.15	170.42	25.40	27.39

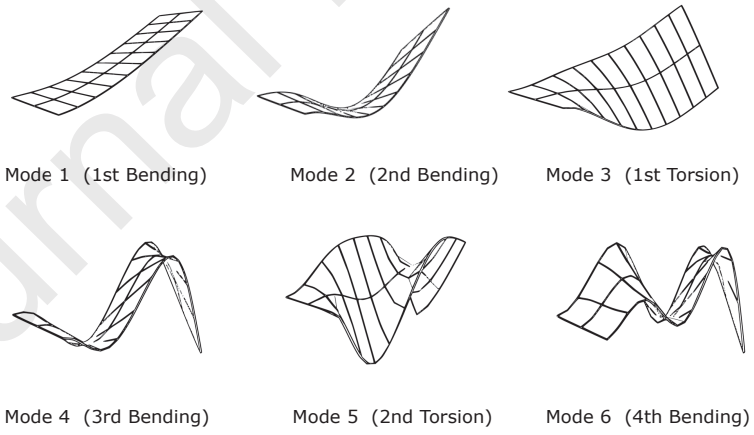

Figure 3: Mode shapes of six-layer plate $[30_2/0]_s$ for LE (2L9) model using CUF.

Another plate model was considered from the Kameyama *et al.* [16] work having eight-layer symmetric laminates [-22.5/67.5/22.5/-67.5]$_s$ with a total thickness of the laminate 0.804 mm. The thicknesses of the plies were 0.037,

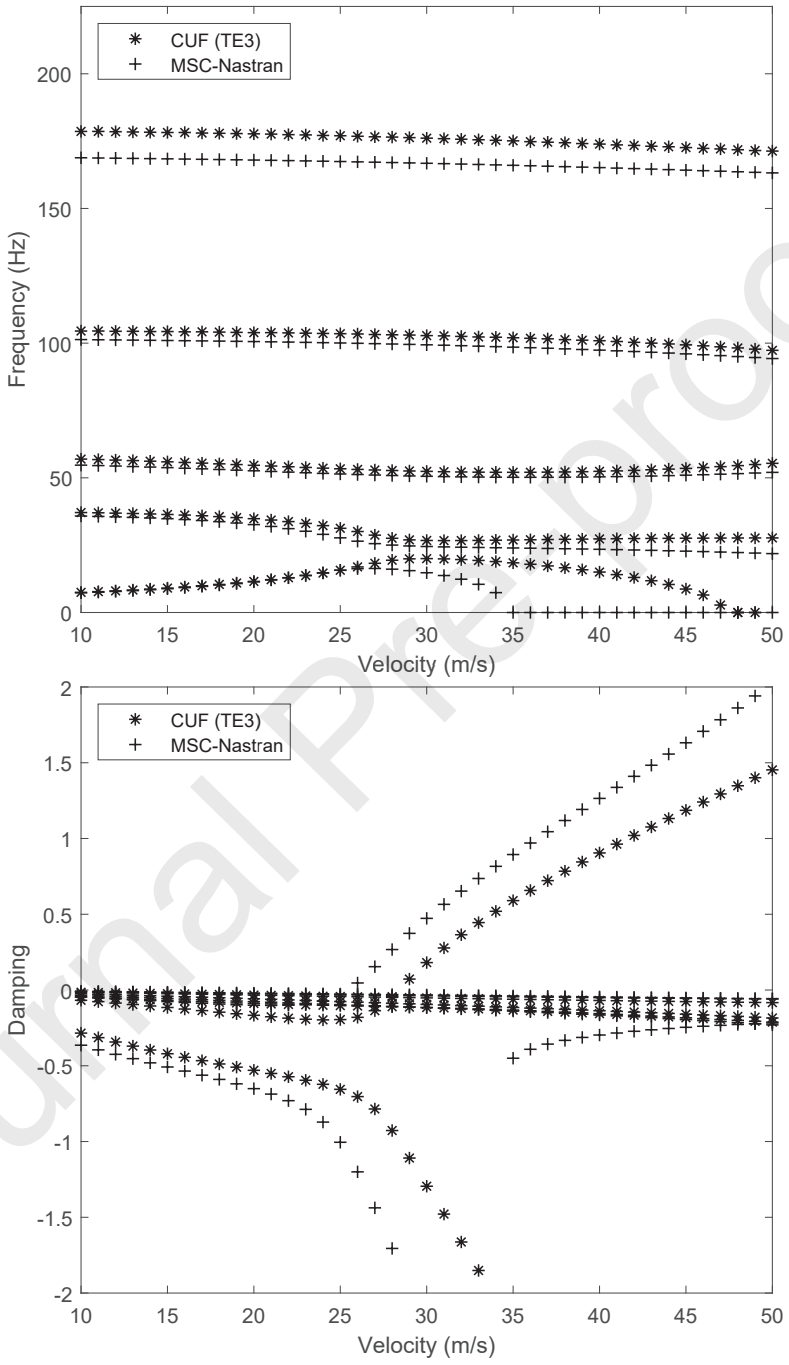

Figure 4: Flutter diagram of orthotropic six-layer plate $[30_2/0]_s$.

Table 4: Natural frequencies (Hz) and flutter conditions for 6-layers plate.

Lamination	Model	Present							Reference	
		f_{n_1}	f_{n_2}	f_{n_3}	f_{n_4}	f_{n_5}	V_F (m/s)	f_F (Hz)	[16] (CLT)	[50] (Exp)
$[0_2/90]_s$	TE3	11.04	39.55	69.16	133.08	193.62	23.20	27.33	23.0	25
	LE (2L9)	11.04	39.51	69.16	132.50	193.62	22.90	27.23		
$[45/-45/0]_s$	TE3	4.88	30.22	50.74	84.59	157.83	47.30	31.48	40.1	>32
	LE (2L9)	4.88	30.10	49.93	84.09	152.84	46.80	31.44		
$[45_2/0]_s$	TE3	5.78	36.60	69.08	103.38	207.51	29.60	25.04	27.5	28
	LE (2L9)	5.78	35.89	68.98	102.78	206.20	29.00	24.93		
$[30_2/0]_s$	TE3	6.31	37.49	57.73	104.65	178.90	27.60	27.22	27.1	27
	LE (2L9)	6.30	37.33	57.11	104.04	174.68	28.10	27.10		

0.048, 0.064 and 0.253 mm, respectively. The first five modes associated with bending and torsion of natural frequency and flutter velocities for CUF model and MSC-Nastran are reported in Table 5. The present results have a good agreement with reference. Similar trends observed like the previous 6-layer plate models. All the TE2, TE3, TE4, 1L9, and 2L9 are suitable, but TE4 and 2L9 are most accurate. Flutter velocity has been found in order with reference results obtained by the generic algorithm for flutter solution, whereas in the present analysis *p-k* method has been used.

Table 5: Natural frequencies (Hz) and flutter condition (velocity [m/s]) for 8-layers plate.

	Model	Mesh	DOFs	f_{n_1}	f_{n_2}	f_{n_3}	f_{n_4}	f_{n_5}	V_f (m/s)
Reference [16]	CLT			7.2	45.4	59.1	127.7	182.3	38.8
Present	TE2	10B4	558	7.3	46.2	59.1	129.8	182.7	38.60
	TE3	10B4	930	7.2	45.1	59.0	126.8	182.5	37.20
	TE4	10B4	1395	7.2	45.1	59.0	126.7	182.3	36.30
	LE (1L9)	10B4	4743	7.2	45.1	59.0	126.8	182.5	38.90
	LE (2L9)	10B4	7905	7.2	45.1	59.0	126.8	182.2	36.80
	MSC-Nastran	10x30	1705	7.2	45.0	58.1	126.2	179.0	35.01

5.3. Box-beam structure

A prismatic thin-walled beam wing model considered for flutter analysis as the main frame of the wing was a box-type structure. A similar

type of analysis on the box-beam was discussed in the introduction section. The dimensions and material properties associated with the composite beam (box-beam) structure are listed in Table 6. The box-beam configuration is shown in Figure 2, where the lamination sequence of four walls, i.e., bottom wall, right wall, top wall and left wall are defined as $[\theta_{bb}/\theta_{rb}/\theta_{tb}/\theta_{lb}]$. The arbitrary lamination sequence $[\theta/0.1\theta/2\theta/10\theta]$ of the walls is considered to avoid the bending-torsion coupling of the structure. In previous sections, it is already observed that TE4 and 2L9 are the more accurate model and the same model in general, is taken here for flutter analysis. In the first case $\theta = 30^\circ$ is considered and the flutter conditions have been computed using CUF and MSC-Nastran model. The first five modes of natural frequencies and flutter conditions (frequency and velocity) are reported in Table 7. The present TE4 and 8L9 results are matching well with the MSC-Nastran. First four modes of frequencies and damping with respect to the function of speed for present TE4 and MSC-Nastran models are shown in Figure 5. The frequency and damping variation with velocity also matching well but with a low computational cost. So, it can be commented that the present models are efficient and accurate and CUF models can be used for flutter analysis of laminated composite box-beam structure. Now, the detailed flutter analysis of various composite box-beam model has been performed by the p-k method. Flutter velocities are computed with variations in θ for different cross-sectional elements and are listed in Table 8. The polar plot for these models is also shown in Figure 6. The polar plot shows that the flutter velocity is increasing between $\theta = 0^\circ$ to $\theta = 30^\circ$ for LE but in TE model case up to $\theta = 60^\circ$. The flutter velocities are reaching a minimum for all the models at $\theta = 90^\circ$. The lower order TE models (i.e., TE2 and TE3) are less effective in predicting flutter conditions comparedto the LE models.In addition, the variations in the computed flutter velocity of theTE model indicate that the higher-order model (TE4) is more effective than lower-order models in determining flutter conditions. It can be observedfrom results that the TE4 and 8L9 models predict the most accurate flutter conditions as compared to other models.

6. Conclusion

Flutter condition of plates and box-beam structures made of isotropic and orthotropic materials has been analyzed in this work. Carrera Unified Formulation (CUF) has been used to define the structural model, one-dimensional

Table 6: Material and dimensional parameter for composite box beam structure.

Material Properties	GPa, kg/m^3
E_{11}	206.8
E_{22}	5.17
$G_{23} = G_{31}$	2.55
G_{12}	3.10
ν_{12}	0.25
ρ	1528.5
Dimensions	m
chord (c)	0.5
height (h)	c / 15
thickness of wall (t)	c / 150
length (L)	3.5

Table 7: Natural frequencies (Hz) and flutter conditions for box-beam ($\theta = 30°$).

Model	Mesh	DOFs	f_{n_1}	f_{n_2}	f_{n_3}	f_{n_4}	f_{n_5}	V_F (m/s)	f_F (Hz)
TE4	10B4	1395	1.80	11.16	23.84	28.46	30.83	105.09	17.52
LE (8L9)	10B4	4464	1.75	10.62	21.55	25.40	28.81	109.10	15.84
MSC-Nastran	5x30(Flange) 3x30(Web)	2480	1.74	10.41	20.73	24.38	26.03	95.09	14.82

Table 8: Flutter condition {velocity (m/s)} for box-beam model.

Model	DOFs	θ=0°	θ=30°	θ=60°	θ=90°	θ=120°	θ=150°	θ=180°
TE2	558	105.4	120.3	122.8	98.9	121.8	118.9	104.5
TE3	930	100.6	114.7	116.2	89.4	105.0	113.0	100.7
TE4	1395	93.0	105.0	109.9	90.2	106.6	110.7	96.6
LE (4L9)	1584	109.5	115.6	110.8	90.8	112.3	114.8	111.0
LE (8L9)	4464	95.4	109.1	100.2	91.9	95.9	106.1	100.5

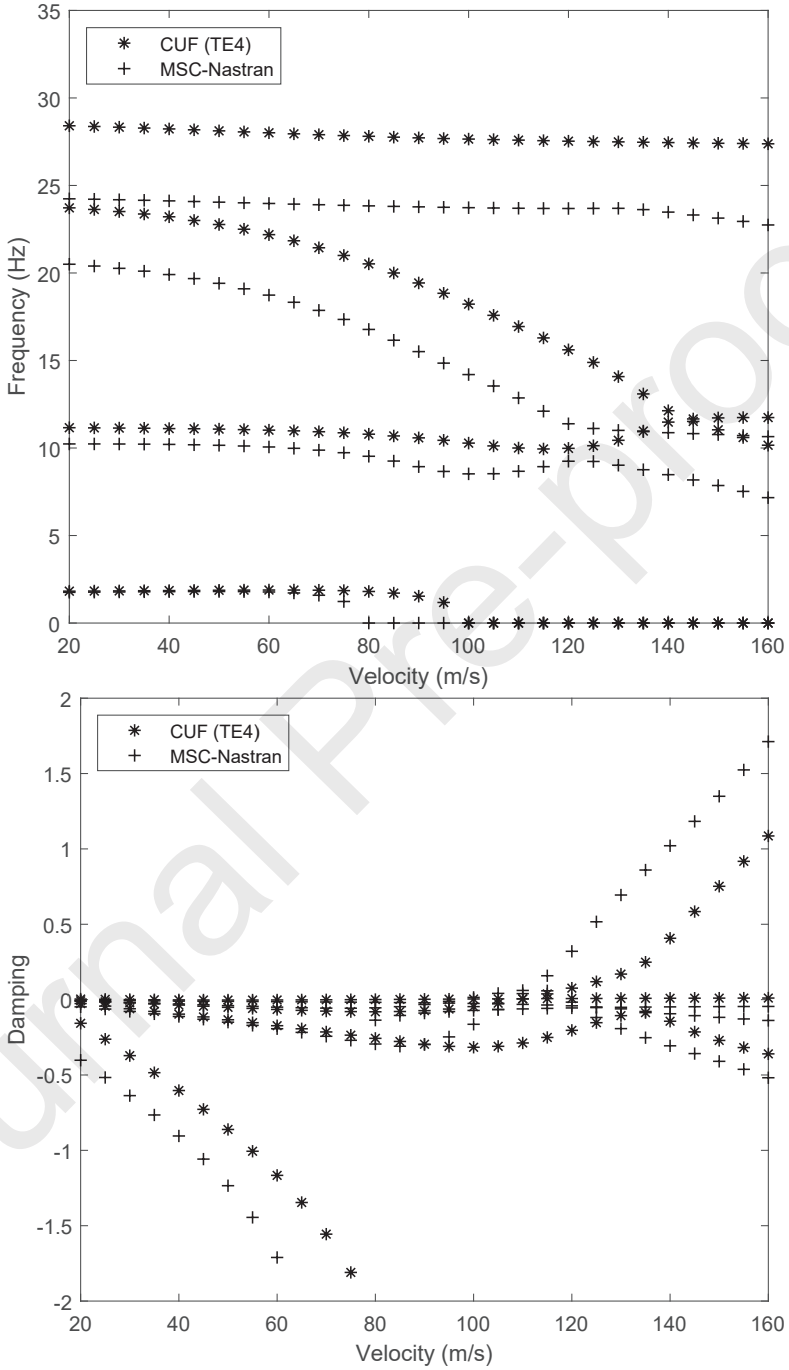

Figure 5: Flutter diagram of box-beam with $\theta = 30°$.

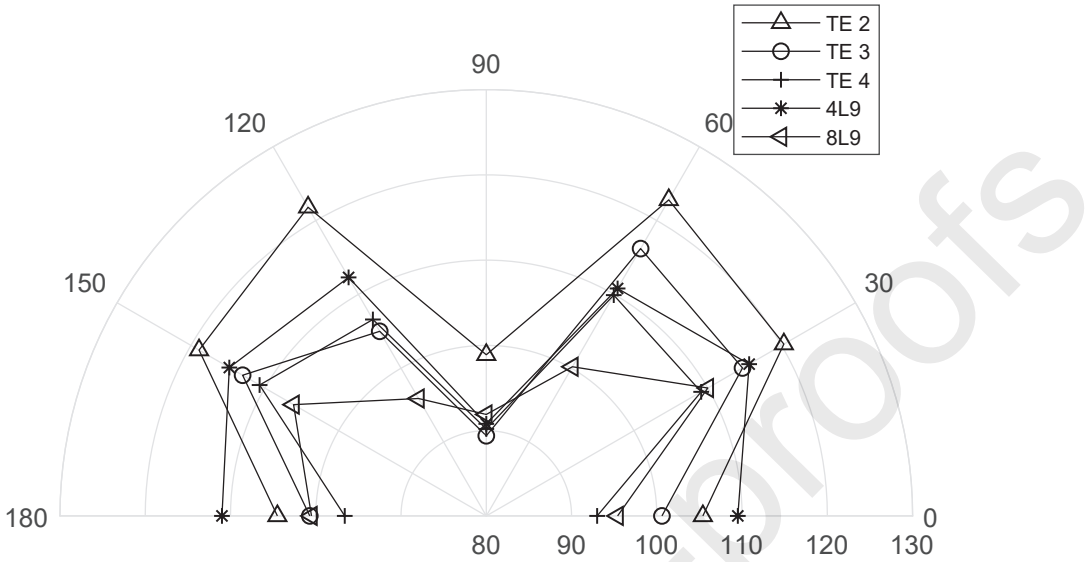

Figure 6: Polar plot of flutter velocities for angle ply of box-beam.

models exploit with Lagrange- and Taylor-like expansions to describe the displacement field of cross-section accurately. The order of Taylor expansion can be chosen arbitrarily in input; it is an independent parameter of the formulation. The governing equation is derived using the principle of virtual displacement and aerodynamic loading conditions are defined in the form of fundamental nuclei in CUF. Furthermore, the p-k method has been implemented and flutter conditions are computed for the unsteady aerodynamics in CUF framework and results have been compared with literature and MSC-Nastran; they are in good agreement. The computed results indicate that for isotropic case, all the TE and LE model can produce good results. Similarly, for the orthotropic plate the TE3, TE4, and 2L9 are preferable to find the flutter conditions. For the composite box-beam, TE4 and 8L9 are the most accurate models. It is also observed that the present TE and LE aeroelastic 1D models are very accurate, efficient with a low computational cost. In the future investigation, aeroelastic analysis of the fixed and rotating-beam models with a quasi-steady and unsteady aerodynamics and gust analysis can be performed in the CUF framework.

Acknowledgement

Authors are thankful to Politecnico di Torino, Italy for providing computational facilities. Bharati RB is thankful to Indian Institute of Technology (ISM), Dhanbad and Ministry of Human Resource Development (MHRD), India for financial support.

References

[1] T. Theodorsen, G. I. E., Mechanism of flutter, a theoretical and experimental investigation of the flutter problem., NACA Report 689, 1940.

[2] T. Theodorsen, G. I. E., General theory of aerodynamic instability and the mechanics of flutter., NACA Report 496, 1949.

[3] D. H. Hodges, G. A. Pierce, Introduction to structural dynamics and aeroelasticity, Vol. 15, cambridge university press, 2011.

[4] H. J. Hassig, An approximate true damping solution of the flutter equation by determinant iteration., J. Aircraft 8 (11) (1971) 885–889.

[5] L. W. Rehfield, A. R. Atigan, D. H. Hodges, Nonclassical behavior of thinwalled composite beams with closed cross sections., J. Amer. Helicopter Soc. 35 (2) (1990) 42–50(9).

[6] X. X. Wu, C. T. Sun, Vibration analysis of laminated composite thinwalled beams using finite elements, AIAA Journal 29 (5) (1991) 736–742.

[7] E. Smith, I. Chopra, Formulation and evaluation of an analytical model for composite box-beams, in: 31st Structures, Structural Dynamics and Materials Conference, 1990.

[8] C. Kim, S. R. White, Thick-walled composite beam theory including 3-d elastic effects and torsional warping, Int. J. Solids Struct. 34 (31) (1997) 4237 – 4259.

[9] V. Berdichevsky, E. Armanios, A. Badir, Theory of anisotropic thinwalled closed-cross-section beams, Compos. Eng. 2 (5) (1992) 411 – 432.

[10] T. A. Weisshaar, Aeroelastic tailoring of forward swept composite wings divergence, Journal of Aircraft 17 (6) (1980) 442–448.

[11] T. A. Weisshaar, Aeroelastic tailoring of forward swept composite wings, Journal of Aircraft 18 (8) (1981) 669–676.

[12] I. Lottati, Flutter and divergence aeroelastic characteristics for composite forward swept cantilevered wing, Journal of Aircraft 22 (11) (1985) 1001–1007.

[13] Z. Qin, L. Librescu, Aeroelastic instability of aircraft wings modelled as anisotropic composite thin-walled beams in incompressible flow, Journal of Fluids and Structures 18 (1) (2003) 43 – 61.

[14] S. Guo, J. Banerjee, C. Cheung, The effect of laminate lay-up on the flutter speed of composite wings, Proceedings of The Institution of Mechanical Engineers Part G-journal of Aerospace Engineering - Proc. Inst. Mech. Eng. G-J A E 217 (2003) 115–122.

[15] S. Guo, W. Cheng, D. Cui, Aeroelastic tailoring of composite wing structures by laminate layup optimization, AIAA Journal 44 (12) (2006) 3146–3150.

[16] M. Kameyama, H. Fukunaga, Optimum design of composite plate wings for aeroelastic characteristics using lamination parameters, Computer Struct. 85 (3) (2007) 213 – 224.

[17] H. Haddadpour, M. Kouchakzadeh, F. Shadmehri, Aeroelastic instability of aircraft composite wings in an incompressible flow, Compos. Struct. 83 (1) (2008) 93 – 99.

[18] R. Firouz-Abadi, A. Askarian, P. Zarifian, Effect of thrust on the aeroelastic instability of a composite swept wing with two engines in subsonic compressible flow, Journal of Fluids and Structures 36 (2013) 18 – 31.

[19] M. R. Catlett, J. M. Anderson, C. Badrya, J. D. Baeder, Unsteady response of airfoils due to small-scale pitching motion with considerations for foil thickness and wake motion, Journal of Fluids and Structures (94) (2020) 102889.

[20] R. Yurkovich, Status of unsteady aerodynamic prediction for flutter of high-performance aircraft, Journal of Aircraft 40 (5) (2003) 832–842.

[21] D. Pitt, A new non-iterative P-K match point flutter solution, 1999.

[22] P. Mahato, D. Maiti, Aeroelastic analysis of smart composite structures in hygro-thermal environment, Compos. Struct. 92 (4) (2010) 1027 – 1038.

[23] E. Carrera, Theories and finite elements for multilayered, anisotropic, composite plates and shells, Archives of Computational Methods in Engineering 9 (2) (2002) 87–140.

[24] E. Carrera, Theories and finite elements for multilayered plates and shells:a unified compact formulation with numerical assessment and benchmarking, Archives of Computational Methods in Engineering 10 (3) (2003) 215–296.

[25] E. Carrera, Assessment of theories for free vibration analysis of homogeneous and multilayered plates, Shock and Vibration 11 (2004) 261–270.

[26] E. Carrera, G. Giunta, Refined beam theories based on a unified formulation, International Journal of Applied Mechanics 2 (2010) 117–143.

[27] E. Carrera, G. Giunta, P. Nali, M. Petrolo, Refined beam elements with arbitrary cross-section geometries, Computers Struct. 88 (5) (2010) 283 – 293.

[28] E. Carrera, M. Filippi, E. Zappino, Free vibration analysis of laminated beam by polynomial, trigonometric, exponential and zig-zag theories, Journal of Composite Materials 48 (19) (2014) 2299–2316.

[29] E. Carrera, M. Filippi, E. Zappino, Laminated beam analysis by polynomial, trigonometric, exponential and zig-zag theories, European Journal of Mechanics - A/Solids 41 (2013) 58 – 69.

[30] E. Carrera, M. Filippi, E. Zappino, Free vibration analysis of rotating composite blades via carrera unified formulation, Composite Structures 106 (2013) 317 – 325.

[31] E. Carrera, E. M. Filippi, E. Zappino, Analysis of Rotor Dynamic by One-Dimensional Variable Kinematic Theories, Journal of Engineering for Gas Turbines and Power 135 (9), 092501.

[32] A. Varello, E. Carrera, L. Demasi, Vortex lattice method coupled with advanced one-dimensional structural models, Journal of Aeroelasticity and Structural Dynamics 2 (2011) 53–78.

[33] A. Varello, A. Lamberti, E. Carrera, Static aeroelastic response of wing-structures accounting for in-plane cross-section deformation, International Journal of Aeronautical and Space Sciences 14 (2013) 310–323.

[34] E. Carrera, A. Varello, L. Demasi, A refined structural model for static aeroelastic response and divergence of metallic and composite wings, CEAS Aeronautical Journal 4 (2) (2013) 175–189.

[35] M. Petrolo, Advanced 1d structural models for flutter analysis of lifting surfaces, International Journal of Aeronautical and Space Sciences 13 (2012) 199–209.

[36] M. Petrolo, Flutter analysis of composite lifting surfaces by the 1d carrera unified formulation and the doublet lattice method, Composite Structures 95 (2013) 539 – 546.

[37] A. Pagani, M. Petrolo, E. Carrera, Flutter analysis by refined 1d dynamic stiffness elements and doublet lattice method, Advances in Aircraft and Spacecraft Science 1 (2014) 291–310.

[38] E. Carrera, E. Zappino, Aeroelastic analysis of pinched panels in supersonic flow changing with altitude, Journal of Spacecraft and Rockets 51 (1) (2014) 187–199.

[39] M. Filippi, E. Carrera, Aerodynamic and mechanical hierarchical aeroelastic analysis of composite wings, Mechanics of Advanced Materials and Structures 23 (2015) 1–31.

[40] E. Carrera, M. Petrolo, Refined one-dimensional formulations for laminated structure analysis, AIAA Journal 50 (1) (2012) 176–189.

[41] E. Carrera, M. Filippi, P. Mahato, A. Pagani, Free-vibration tailoring of single- and multi-bay laminated box structures by refined beam theories, Thin-Walled Structures 109 (2016) 40 – 49.

[42] I. Kaleel, M. Petrolo, A. Waas, E. Carrera, Computationally efficient, high-fidelity micromechanics framework using refined 1d models, Composite Structures 181 (2017) 358 – 367.

[43] E. Carrera, E. Zappino, One-dimensional finite element formulation with node-dependent kinematics, Computer Struct. 192 (2017) 114 – 125.

[44] R. B. Bharati, P. K. Mahato, E. Carrera, M. Filippi, A. Pagani, Free Vibration and Stress Analysis of Laminated Box Beam with and Without Cut-Off, Recent Advances in Theoretical, Applied, Computational and Experimental Mechanics, 2020, pp. 185–196.

[45] A. H. Bisplinghoff R. L., H. R. L., Aeroelasticity., Dover Publication Inc, New York, 1996.

[46] R. T. Jones, Operational treatment of the nonuniform-lift theory in airplane dynamics., Technical Report 667, NASA, 1938.

[47] E. Carrera, M. Filippi, P. K. Mahato, A. Pagani, Advanced models for free vibration analysis of laminated beams with compact and thin-walled open/closed sections, J. Compos. Mater. 49 (17) (2015) 2085–2101.

[48] SIEMENS: Aeroelastic AnalysisUser's Guide (2014).

[49] M. Petrolo, Advanced aeroelastic models for the analysis of lifting surfaces made of composite materials, Ph.D. thesis, PhD. Dissertation, Politecnico di Torino, Turin, Italy (2011).

[50] S. J. Hollowell, J. Dugundji, Aeroelastic flutter and divergence of stiffness coupled, graphite/epoxy cantilevered plates, Journal of Aircraft 21 (1) (1984) 69–76.